

**CHARACTERIZATION OF THE SANDWICH-TYPE
BEAM WITH DOUBLE PIEZOELECTRIC MATERIALS
USING ANSYS SOFTWARE**

By:

NUR AZIMA BINTI AZIZ JAAFAR

(Matric no.:120405)

Supervisor:

DR AHMAD ZHAFRAN BIN AHMAD MAZLAN

June 2017

This dissertation is submitted to
Universiti Sains Malaysia
As partial fulfillment of the requirement to graduate with honors degree in
BACHELOR OF ENGINEERING (MECHANICAL ENGINEERING)



School of Mechanical Engineering
Engineering Campus
Universiti Sains Malaysia

DECLARATION

I hereby declare that the work reported in this thesis is the result of my own investigation and that no part of the thesis has been plagiarized from external sources. Materials taken from other sources are duly acknowledged by giving explicit references.

Signature:

Name of student: NUR AZIMA BINTI AZIZ JAAFAR

Matrix number: 120405

ACKNOWLEDGMENT

The completion on this undertaking could not have been possible without the participation and assistance of so many people whose name may not all be enumerated. Their contributions are sincerely appreciated and gratefully acknowledged.

Praised be to the Almighty Allah Subhanahu Wataalla, the Most Gracious the Most Merciful, for the patience, knowledge and courage.

Dr. Ahmad Zhafran Ahmad Mazlan, my supervisor, for the encouragement, guidance and suggestions throughout this research. Without him, this research will not be the same as presented here.

Besides that, a special thanks to my friends, Farah Naimah Rogaizat, Farhana Mohamad Fathi and Siti Nuraimi Abdul Hamid for their constant help and support throughout the completion of this research.

Last but not least, I place on record my sense of gratitude to one and all who in one way or another shared their support, either morally, physically, and financially.

Thank you.

TABLE OF CONTENTS

DECLARATION	I
ACKNOWLEDGMENT	II
LIST OF TABLES	V
LIST OF FIGURES	VI
NOMENCLATURE.....	VIII
ABSTRAK	IX
ABSTRACT	X
CHAPTER 1: INTRODUCTION	1
1.1. Overview	1
1.2. Background study	1
1.3. Problem statement	2
1.4. Objective.....	2
1.5. Scope	2
CHAPTER 2: LITERATURE REVIEW	3
2.1. Overview	3
2.2. Piezoelectric material and its application as sensor and actuator	3
2.3. Piezoelectric non-linear characteristics and its compensation method	4
2.4. Modelling of piezoelectric patches using FEM	5
2.5. Summary.....	6
CHAPTER 3: METHODOLOGY	7
3.1. Overview	7

3.2. Piezoelectric patch specification	7
3.3. Modelling of piezoelectric patch using ANSYS software.....	8
3.4. Beam characterization	10
3.4.1. Modal analysis.....	10
3.4.2. Harmonic response analysis	12
3.4.3. Transient structural analysis with input forces.....	13
3.5. Piezoelectric actuator characterization	14
CHAPTER 4: RESULTS AND DISCUSSION.....	17
4.1. Overview	17
4.2. Beam characteristics	17
4.2.1. Beam.....	17
4.2.2. Beam with piezoelectric patches	23
4.3. Piezoelectric actuator characteristics.....	30
CHAPTER 5: CONCLUSION.....	34
5.1. Conclusion	34
5.2. Scope of future work	34
REFERENCES.....	36

LIST OF TABLES

	Page
3.1 Piezoelectric patch specification	8
3.2 Aluminium alloy properties	11
3.3 Piezoelectric material properties	11
3.4 The details analysis setting of harmonic response	13
4.1 Natural frequencies of the beam	17
4.2 Natural frequencies of the beam with piezoelectric patches	24

LIST OF FIGURES

	Page
2.1 The different location of the piezoelectric patch on the beam structure	5-6
3.1 The picture and detail dimensions of piezoelectric patch	7
3.2 The available beam with piezoelectric patch sensor and actuator	9
3.3 The different views of the beam with piezoelectric patch sensor and actuator	9
3.4 Configuration of the beam structure	10
3.5 The meshed model of beam and piezoelectric patches	11
3.6 The schematic diagram and outline of modal and harmonic response analyses	12
3.7 The harmonic response analysis setup	13
3.8 The Transient structure analysis setup	13
3.9 Transient structure analysis schematic diagram and project outline	14
3.10 The surface nodes selection on the piezoelectric actuator	15
3.11 Project outline for piezoelectric actuator transient analysis	16
4.1 Mode shapes of the beam	18
4.2 FRF of (a) displacement (b) velocity and (c) acceleration of the beam	18-19
4.3 FFT acceleration of the beam with input forces at frequency (a) 100Hz (b) 200Hz (c) 300Hz (d) 400Hz and (e) 500Hz	20-22
4.4 The deflection of the beam at 300 Hz for input force 1 N	
4.5 The results of acceleration of the beam at different operating frequencies and excitation forces	23
4.6 Mode shapes of the beam with piezoelectric patches	24
4.7 FRF of (a) displacement (b) velocity and (c) acceleration of the beam with piezoelectric patches	25

4.8	The FFT of acceleration with input forces at frequency (a) 100Hz (b) 200Hz (c) 300Hz (d) 400Hz and (e) 500 Hz of the beam with piezoelectric patches	26-28
4.9	The deflection of the beam at 300 Hz with input force 1 N	29
4.10	The results of acceleration of the beam with piezoelectric patches at different operating frequencies and excitation forces	29
4.11	The FFT of acceleration with input voltage to the piezoelectric patch at frequency (a) 100Hz (b) 200Hz (c) 300Hz (d) 400Hz and (e) 500Hz of the beam	30-32
4.12	The deflection of beam structure at 500 Hz with input voltage 100 V	33
4.13	The results of acceleration of the beam with piezoelectric patches at different operating frequencies and excitation voltage on the actuator	33

NOMENCLATURE

Symbols	Descriptions
AVC	Active vibration control
FEM	Finite element method
FEA	Finite element analysis
LTI	Linear time invariant
FRF	Frequency response function
EM	Electro-mechanical
FE	Finite element
FFT	Fast Fourier transform

ABSTRAK

PENCIRIAN RASUK JENIS SANDWICH DENGAN BAHAN PIEZOELEKTRIK BERKEMBAR MENGGUNAKAN PERISIAN ANSYS

Dalam kajian ini, ciri-ciri rasuk aluminium jenis sandwich dengan sepasang piezoelektrik tampalan telah disiasat. Kajian ini menggunakan perisian ANSYS-16 sebagai platform untuk memperolehi model unsur terhingga rasuk jenis sandwich. Dua kes kajian telah disiasat untuk ciri-ciri rasuk iaitu bagi rasuk tunggal dan rasuk dengan piezoelektrik tampalan. Pertama sekali, analisis modal telah dijalankan, dan empat frekuensi semula jadi telah ditentukan bagi kedua-dua kes. Seterusnya, analisis fana dilakukan dengan menggunakan pengujaan kuasa gelombang sinus di tepi hujung kanan rasuk. Analisis ini dijalankan untuk julat frekuensi 0-500 Hz. Keputusan menunjukkan bahawa rasuk cenderung untuk bertindak balas pada frekuensi semula jadi apabila frekuensi pengujaan hampir kepada frekuensi semula jadi struktur rasuk. Ciri-ciri piezoelektrik tampalan sebagai penggerak juga dianalisis dengan menggunakan pengujaan voltan gelombang sinus pada piezoelektrik tampalan. Keputusan menunjukkan bahawa bahan piezoelektrik tampalan mempunyai kemungkinan untuk digunakan sebagai penggerak bagi mengurangkan getaran struktur rasuk.

ABSTRACT

CHARACTERIZATION OF THE SANDWICH-TYPE BEAM WITH DOUBLE PIEZOELECTRIC MATERIAL USING ANSYS SOFTWARE

In this study, the characteristics of the sandwich-type aluminium beam with one pair of piezoelectric patches are investigated. The study uses ANSYS-16 software as a platform to create the finite element (FE) model of the sandwich-type beam. Two case studies are investigated for beam characteristics which are the single beam and beam with piezoelectric patches. Firstly, the modal analysis has been carried out, and four natural frequencies have been determined for both cases. Then, the transient analysis is done by applying the sine wave force excitation at the edge of the right-end of the beam. The analysis is carried out for the frequency range of 0-500 Hz. The results show that, the beam is tending to excite at the natural frequencies when the excitation frequencies are closed to the natural frequencies of the beam structure. The characteristic of the piezoelectric patch as an actuator is also analyzed by applying sine wave voltage excitation to the piezoelectric patch. The results show that, the piezoelectric patch material has the possibility to be used as an actuator to reduce the vibration of the beam structure.

CHAPTER 1: INTRODUCTION

1.1. Overview

This chapter presents background study, problem statement, objective, and scope of the study.

1.2. Background study

Piezoelectric material is a dielectric material that belongs to the class of non-centrosymmetric crystals. When these materials are subjected to an external electric field, there will be asymmetric displacements of anions and cations that cause considerable net deformation of the crystal (Vijaya 2013).

The word Piezoelectricity comes from Greek *piezin* which means pressure electricity. This word was proposed by Hankel in 1881 to name the phenomenon discovered a year before by Curie brothers. They observed that positive and negative charges appeared on several parts of the crystal surfaces when comprising the crystal in different direction (Arnau and Soares 2008). In 1881, mathematician Gabriel Lippmann demonstrated that there should be a converse piezoelectric effect, where by applying an electric field to a crystal should can cause material to deform in response. The Curies immediately confirmed the existence of the "converse effect," and continue to obtain quantitative proof of the complete reversibility of electro-elasto-mechanical deformations in piezoelectric crystals (Piezo Systems 2011).

Piezoelectric materials are widely used as distributed sensors and actuators for many active vibration control (AVC) applications. To design piezoelectric for AVC, both structural dynamic and control theory need to be considered. Finite element method (FEM) is one of the powerful tool for analyzing complex structures, which capable in dealing with the piezoelectric structures. Among the commercially available finite element analysis (FEA) codes, ANSYS, has the ability to model the piezoelectric materials (Dong, Meng et al. 2006).

1.3. Problem statement

Piezoelectric actuators have attracted considerable interest because of its characteristics which can be used in many applications such as AVC. A lot of researchers have been solving the limitation of the piezoelectric actuator over the past year with different type of solutions including using the FEM. Therefore, the characteristic of piezoelectric actuator (i.e. piezoelectric patch) together with the flexible structure is studied using the FEM to further understand the behaviors of this material and its effect to the structure.

1.4. Objective

In this study, two objectives are set to be achieved:

1. To develop a sandwich-type beam with double piezoelectric materials (sensor and actuator) using ANSYS software.
2. To characterize the beam and piezo patch actuator using ANSYS software.

1.5. Scope

This work focused in developing the sandwich-type beam with double piezoelectric patch material using FEM (i.e. ANSYS) software. Next, the characteristics of the beam and piezoelectric patch are observe using this software.

CHAPTER 2: LITERATURE REVIEW

2.1. Overview

In this chapter, three main areas are presented, including the piezoelectric material applications, characteristics and compensation methods and modelling of piezoelectric using FEM.

2.2. Piezoelectric material and its application as sensor and actuator

Piezoelectric materials have been known because of their potential as smart materials. This material has inherent transducer characteristics which capable to become both sensor and actuator. It convert the mechanical energy to an electrical energy (i.e., direct piezoelectric effect) and electrical energy to mechanical energy (indirect piezoelectric effect) (Vijaya 2013).

The piezoelectric constitutive equations in the stress-charge form are given by:

$$\sigma = c_E S - e_p E_e \quad (1)$$

$$D_e = e_p^T S + \epsilon_S E_e \quad (2)$$

Where S is strain, σ is stress, D_e is the electric displacement, E_e is the electric field strength, e_p are the piezoelectric coupling coefficients in the stress-charge form, c_E contains stiffness coefficients under constant electric field and ϵ_S is the electric permittivity matrix under constant strain. Subscripts E indicates zero or constant electric field and σ is zero or constant stress field, while superscript T denotes matrix transposition (Takács and Rohal-Ilkiv 2012).

Piezoelectric materials have been applied in many applications such as for engineering and medical solutions because it has variety of properties, which are superior comparing to other materials. Piezoelectric actuators have recently attracted considerable interest due to the wideband, simple, reliable, compact, and lightweight characteristics (Preumont, Dufour et al. 1992). Piezoelectric actuators can produce quick accurate movements which is preferable in many applications.

The applications of piezoelectric material as actuator and sensor have been studied before. One of the application is a piezoelectric based built-in diagnostic technique which has been developed for monitoring fatigue crack growth in metallic structures. The technique uses diagnostic signals which generated from the nearby piezoelectric actuators and built into the structures to detect crack growth.

2.3. Piezoelectric non-linear characteristics and its compensation method

Piezoelectric actuator is a device that uses inverse piezoelectric effect (electric charge to mechanical stress). However, in some cases it is practically insufficient due to the small displacement even though under high voltage driven. The piezoelectric actuators must be structurally processed in order to obtain a larger displacement output from a low driven voltage and the process has thus been put to practical use (Yoichi 2006).

The applications of piezoelectric actuators are restricted by their nonlinearity behaviors, such as hysteresis and creep (Zhao, Zhang et al. 2013). In simple terms, hysteresis means that for a certain input, there is no unique output. Instead, the output depends on the input history (Adriaens, de Koning et al. 2000). Meanwhile, creep describes the change in the displacement over time with an unchanged drive voltage. The creep speed decreases logarithmically over time. Basically, hysteresis has a bigger influence on piezoelectric actuators performance than creep, but creep can deteriorate the positioning accuracy over the extended period of time.

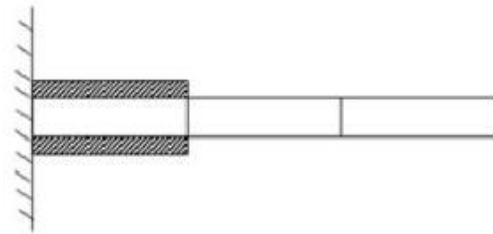
There are two methods that can be applied to compensate the creep effect. Firstly, the effect can be suppressed using complex algorithms in the closed-loop arrangement. However, this method requires expensive devices in order to achieve fast data acquisition and high-speed computation. Secondly, their inverse models can be applied to compensate the creep effect. Some phenomenological creep models were used in the open loop, such as log-type and linear time invariant (LTI). However, the parameters in these models are complex and hysteretic (Zhao, Zhang et al. 2013).

For the of nonlinear hysteresis effect, it can be corrected using the charge controller. However, charge controller is inherently bulky, costly, and has limited sensitivity. It may lead to drift and saturation problems and reduces the operating range

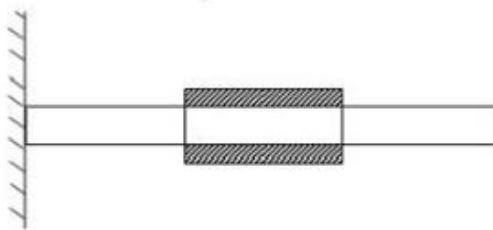
of the piezoelectric actuator. Consequently, a voltage control strategy for piezoelectric actuator proves to be more promising, economical and commercially acceptable solutions. Several hysteresis models have been utilized by various researches. The hysteresis models can be divided into mathematical model and nonlinear differential model. A nonlinear differential model used with time varying coefficients to approximate the hysteresis nonlinearity effects in the piezoelectric actuator. Then a sliding mode control can be used to achieve the insensitivity against parameter uncertainties (Najafabadi, Rezaei et al. 2007).

2.4. Modelling of piezoelectric patches using FEM

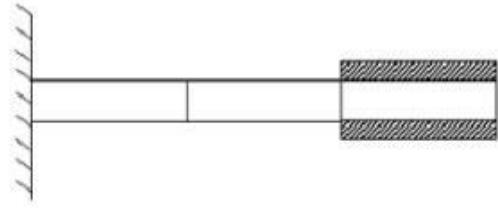
There is a study using a beam like structures with distributed piezoelectric actuator and sensor as shown in Figure 2.1 (a-c). In these figures, both piezoelectric are layers bonded on top and bottom surfaces of the beam which the piezoelectric patch are located at different positions to determine better control effect (Chhabra, Narwal et al. 2012).



(a) Piezoelectric placed at the fixed end



(b) Piezoelectric placed at the middle



(c) Piezoelectric placed at the free end

Figure 2.1: (a) ~ (c) The different location of the piezoelectric patch on the beam structure

In their study, the responses of the various locations of sensor and actuator on the beam have been observed and the best performance is obtained when the piezoelectric element is placed at fixed end position (Figure 2.1 (a)), where the settling time become faster as the patches are put closer to the fixed end (Chhabra, Narwal et al. 2012).

In this case, numerical approach such as FEM will be sought for acceptable solutions. Piezoelectric elements have now included in the commercial finite element codes such as ANSYS and ABAQUS (Xu and Koko 2004). To design piezoelectric smart structures for AVC system, both structural dynamics and control theory need be considered.

2.5. Summary

All the three main topics that related to the piezoelectric material, piezoelectric characteristics and FEM analysis have been discussed in this chapter. From these, it can be summarized that:

- (a) There are several studies used an ANSYS Mechanical APDL to analyze the model but rarely been studied using ANSYS Mechanical Workbench.
- (b) The characterization of piezoelectric as an actuator is limited only for constant voltage input.

CHAPTER 3: METHODOLOGY

3.1. Overview

In this chapter, the methodology of the research is presented, including the piezoelectric patch specification, modelling of the beam with piezoelectric patch using ANSYS and the details of analysis including the modal, harmonic and transient analyses of the structure.

3.2. Piezoelectric patch specification

In this study, a piezoelectric patch transducer (P-876 DuraAct™) was used to represent the actuator and sensor for the AVC system. Figure 3.1 shows the picture and the detail dimensions of the piezoelectric patch. From the figure, the overall shape of the piezoelectric patch consists of electrode plate that is coated with piezoceramic layer on each side of the plate and the external body of the piezoelectric patch is laminated with polymer which provides a mechanically preloaded and electrically insulated device. The detail of piezoelectric patch specification is listed in Table 3.1.

*All dimensions are in mm

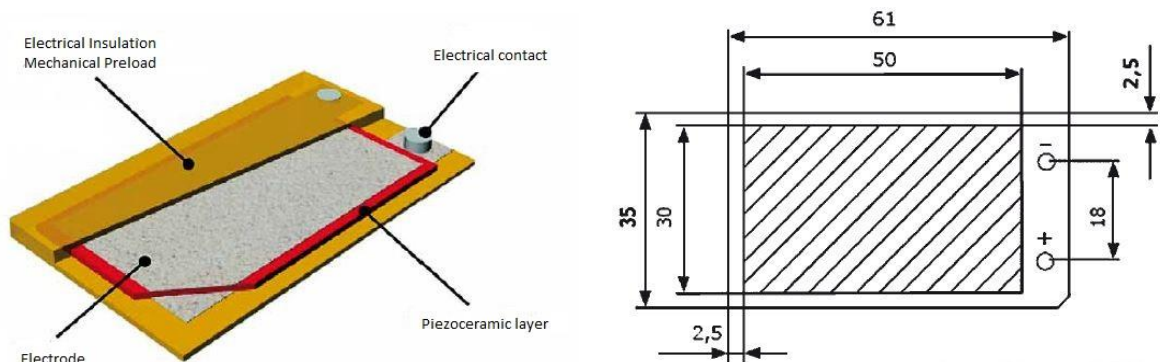


Figure 3.1: The picture and detail dimensions of piezoelectric patch ((PI 2015)

Table 3.1: Piezoelectric patch specification ((PI) 2015)

Parameter	Value
Model	P-876.A15
Operating voltage	-250 to +1000 V
Lateral contraction, open-loop	900 $\mu\text{m}/\text{m}$, 0,64 $\mu\text{m}/\text{mN}$
Blocking force	775 N
Dimensions	61 x 35 x 0.8 mm
Bending radius	70 mm
Ceramic type	PIC 255
Piezoceramic height	500 μm
Electrical capacitance	45 nF
Operating temperature range	-20 to +150
Mass	7.2 g
Voltage connection	Soldering pads
Recommended controller/amplifier	E-508 (s.p. 2-150) E-835 (s.p. 2-166)

3.3. Modelling of piezoelectric patch using ANSYS software

A sandwich-type beam with double piezoelectric patch material (sensor and actuator) was drawn using the ANSYS DesignModeler (ANSYS Inc.). The dimension of the beam (40 mm x 180 mm x 1 mm) was first measured and drawn using this software. Figure 3.2 shows the available beam with piezoelectric patch sensor and actuator. The beam is attached with the piezoelectric patch at the top and bottom which act as a sensor and actuator respectively. Figure 3.3 shows the drawing of top, side and isometric views of the aluminium beam with piezoelectric patch sensor and actuator.

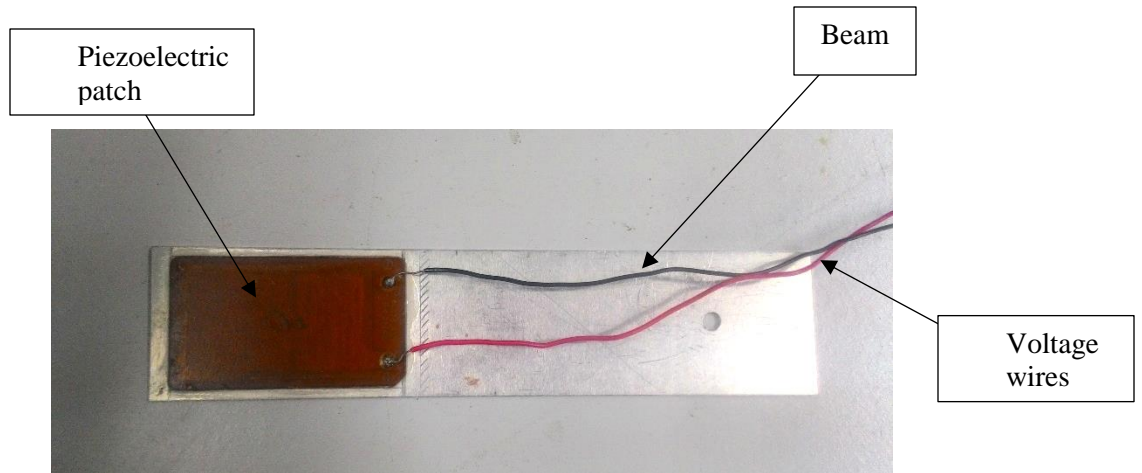
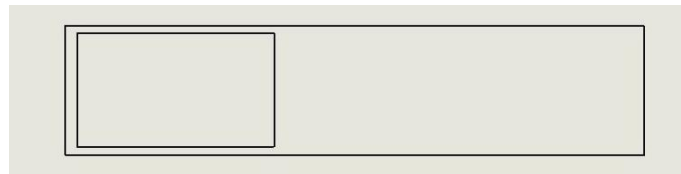
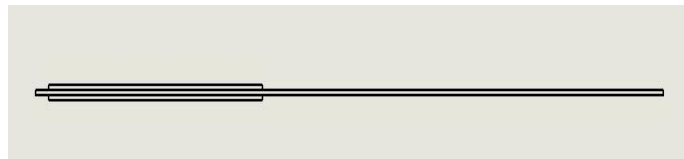


Figure 3.2: The available beam with piezoelectric patch sensor and actuator

(a) Top view



(b) Side view



(c) Isometric view

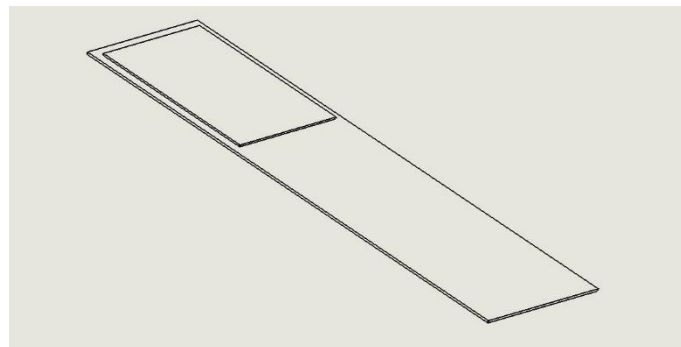


Figure 3.3: (a) ~ (c) The different views of the beam with piezoelectric patch sensor and actuator

3.4. Beam characterization

The characterization of the beam is carried out in two ways which are beam and beam with piezoelectric patches.

3.4.1. Modal analysis

In this section, the modal analysis of the sandwich-type beam with dual piezoelectric patch is simulated using Workbench ANSYS software. Apparently, the goal of modal analysis is to determine the natural frequencies and mode shapes of the structure (Wu, Li et al. 2013). The configuration of the beam structure for modal analysis is shown in Figure 3.4.

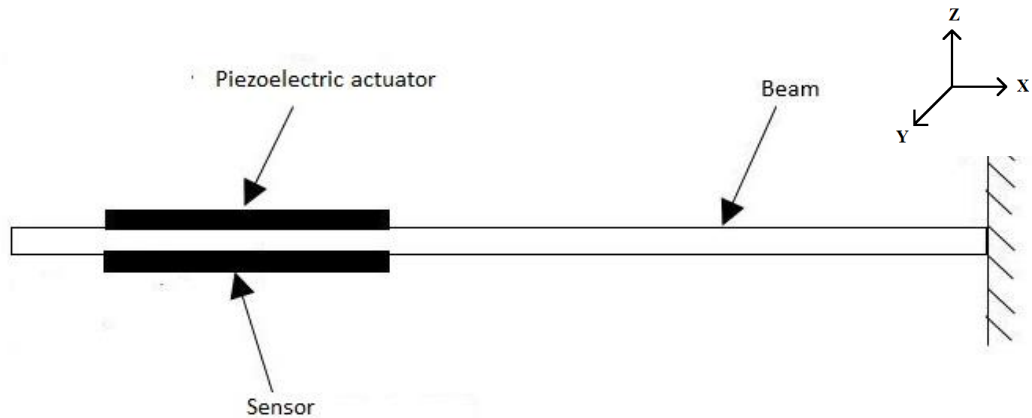


Figure 3.4: Configuration of the beam structure

The material properties of the beam and the piezoelectric patches were first selected from the engineering data library. An aluminium alloy is assigned for the beam and the piezoelectric material is assigned for the piezoelectric patches. The available piezoelectric patch is a navy type II (PZT-5A) ceramic. Therefore, the stiffness matrix of PZT-5A is used for the anisotropic elasticity property. Table 3.2 and Table 3.3 show the list of aluminium alloy and piezoelectric material properties respectively.

Table 3.2: Aluminium alloy properties (ANSYS Inc.)

Property	Value
Density	2770 kg/m ³
Isotropic elasticity:	
1. Young's modulus, E	71000 MPa
2. Poisson's ratio, ν	0.33
3. Bulk modulus, E _b	69600 MPa
4. Shear modulus, E _s	26692 MPa

Table 3.3: Piezoelectric material properties (Nader, Silva et al. 2003)

Property	Value
Density	7750 kg/m ³
Anisotropic elasticity	Stiffness matrix Compliance, C
	$= \begin{bmatrix} 12.1 & & & & & & \\ 7.54 & 11.1 & & & & & \\ 7.52 & 7.24 & 12.1 & & & & \\ 0 & 0 & 0 & 2.11 & & & \\ 0 & 0 & 0 & 0 & 2.11 & & \\ 0 & 0 & 0 & 0 & 0 & 2.26 & \end{bmatrix} \times 10^{10} Pa$

The beam and piezoelectric patches structure are meshed with mesh size of 0.0025m and a fixed support was set at the right -end of the beam. The meshed model of the structure is illustrated in Figure 3.5. For this analysis, a limit range of frequency is set from minimum frequency of 0 Hz to maximum frequency of 500 Hz.



Figure 3.5: The meshed model of beam and piezoelectric patches

3.4.2. Harmonic response analysis

Harmonic response analysis is a technique used to determine the steady-state response of a linear structure with loads and varies harmonically with time (ANSYS Inc.). Basically, this analysis is carried out to gain the frequency response function (FRF) of the structure. Results from the modal analysis are used in this harmonic response analysis. This method is called mode superposition which is sums factored mode shapes (Nie and Wei 2011). Figure 3.6 illustrated the schematic diagram of the modal and harmonic responses connection and the outline of harmonic response analysis.

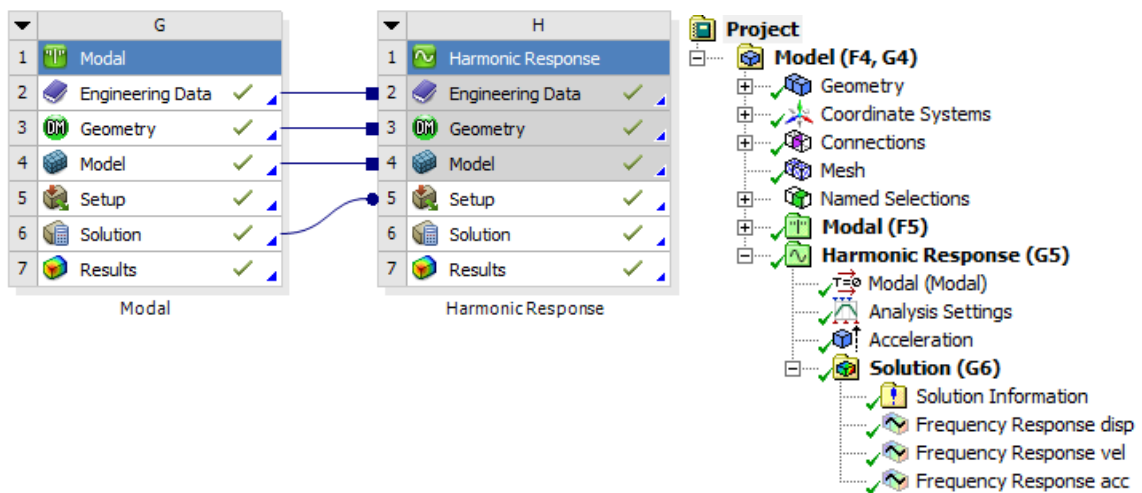


Figure 3.6: The schematic diagram and outline of modal and harmonic response analyses

In order to solve the study, at least a single load is needed. As for this analysis, an acceleration of 9.81 m/s^2 is applied at the center of the body. Figure 3.7 shows the setup of the structure in harmonic response analysis. The details of the analysis setting are tabulated in Table 3.4. The outcomes from this analysis are used as a guide to ensure that the transient analysis results are acceptable.

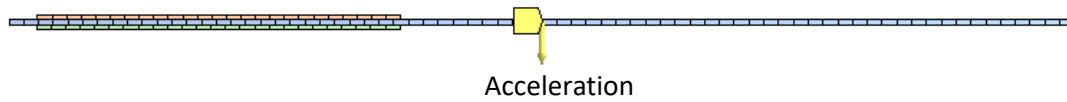


Figure 3.7: The harmonic response analysis setup

Table 3.4: The details analysis setting of harmonic response

Options	
Frequency spacing	Linear
Range minimum	0 Hz
Range maximum	500 Hz
Solution intervals	100
Solution method	Mode superposition

3.4.3. Transient structural analysis with input forces

Transient structural analysis is a technique used to determine the dynamic response of a structure under a time-varying load (Alberta 2001). The external input force, F is applied at the edge on the left-end of the beam in z -axis direction as shown in Figure 3.8. For the analysis of beam with piezoelectric patches, the actuator is added with piezoelectric and MEMs body extension which defined as piezoelectric body.

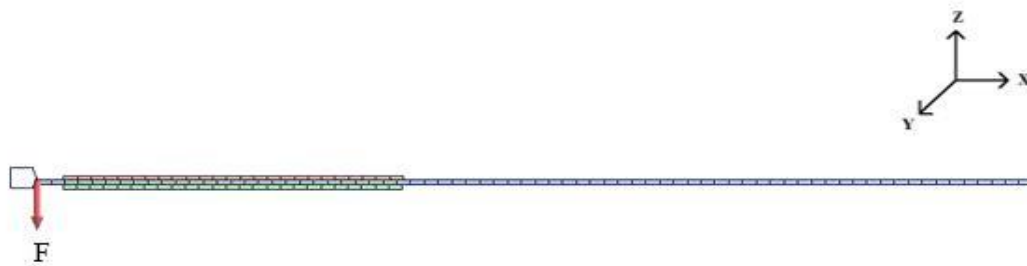


Figure 3.8: The Transient structure analysis setup

The sinusoidal input force is calculated from equation below:

$$F = F_0 \sin \omega t \tag{3}$$

Where $F_0 = 1, 2, 3, 4, \text{ and } 5 \text{ N}$

$$\omega = 2\pi f \text{ , } f = 100, 200, 300, 400, \text{ and } 500 \text{ Hz}$$

The value of time step, Δt used for this analysis is 0.0005s with step end time of 0.2s. In this analysis, the deformation (i.e, displacement), velocity and acceleration of the beam are identified. As the results encountered minimum and maximum values, probe reaction feature is used. Probe reaction allow the display of the result probe to reveal the displaced mesh for the specified time (ANSYS Inc.). Figure 3.9 shows the transient analysis schematic diagram and project outline

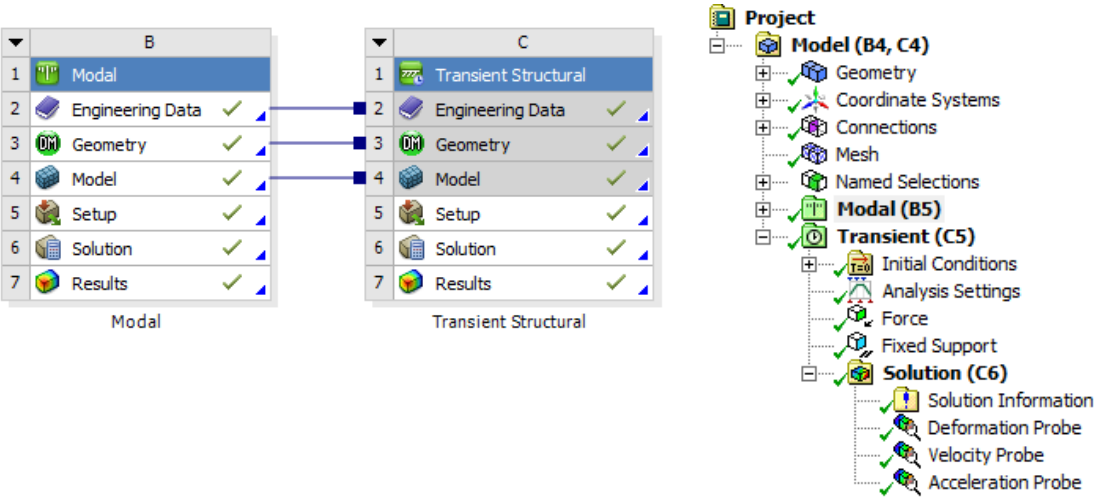


Figure 3.9: Transient structure analysis schematic diagram and project outline

3.5. Piezoelectric actuator characterization

The characterization of piezoelectric actuator is carried out using transient structural analysis module. A sinusoidal input voltage is applied on the surface of the actuator to excite the piezoelectric patches with the beam structure. In this case, an electro-mechanical (EM) transducer of Direct Finite Element (FE) group feature is used. The Direct FE features allow you to apply boundary conditions directly to the nodes on the finite element mesh of a model (ANSYS Inc.). EM transducers can convert the

electrical energy to the mechanical stress and vice versa, and this is mostly nonlinear in nature (Safari and Akdogan 2008) . In this case, piezoresistivity body is used to added electrical properties in the actuator.

For the ANSYS Mechanical APDL, in order to set the boundary condition, EMTGEN command is used to generate a set of TRANS126 element between the surface nodes of a movable structure and a plane of nodes (ground plane). Therefore, the most important step is the selection of surface nodes which is on the top surface of the actuator. Figure 3.10 illustrated the nodes selection on the surface of the actuator. The initial gap which is the gap between actuator and the beam was set to 0.0001m in z-direction.

The value of voltage input, V is calculated using equation below:

$$V = V_o \sin\omega t \quad (4)$$

Where $V_o = 100, 200, 300, 400, \text{ and } 500 \text{ V}$

$$\omega = 2\pi f \text{ , } f = 100, 200, 300, 400, \text{ and } 500 \text{ Hz}$$

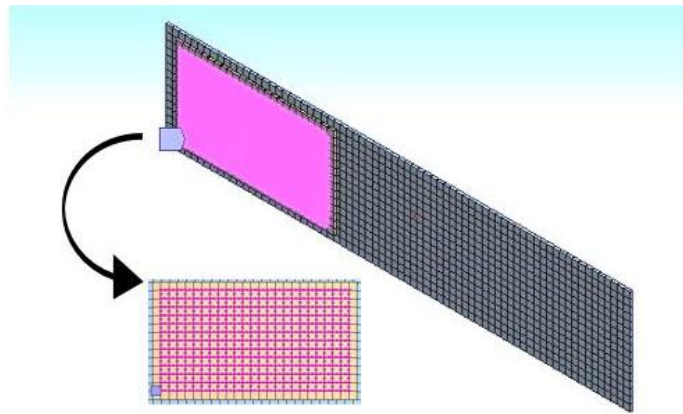


Figure 3.10: The surface nodes selection on the piezoelectric actuator

In this study, same Δt is used which is 0.0005s with step end time of 0.2s. The solution results of the displacement, velocity and acceleration in z-direction is determined. Figure 3.11 shows the outline of the piezoelectric actuator transient analysis.

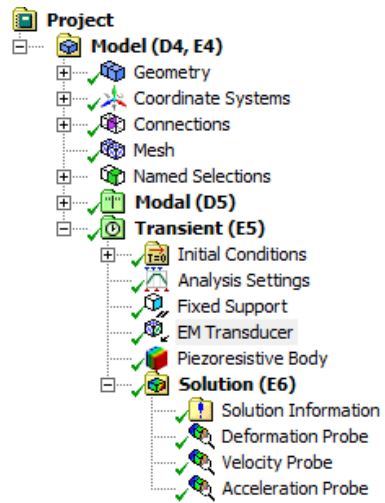


Figure 3.11: Project outline for piezoelectric actuator transient analysis

CHAPTER 4: RESULTS AND DISCUSSION

4.1. Overview

In this chapter, the simulation results are presented which includes the characteristics of the beam alone and beam with piezoelectric material and piezoelectric patches as an actuator.

4.2. Beam characteristics

In this section, the beam characterization is presented, including a single beam and a beam with piezoelectric patches.

4.2.1. Beam

4.2.1.1 Modal and harmonic response analysis

The results from the modal analysis are tabulated on Table 4.1 and Figure 4.1 illustrated the mode shapes of the beam. From these results, the natural frequencies of the beam for frequency range of 0 – 500 Hz which four mode shapes are shown. The first natural frequency of 26.00 Hz as (1st bending) is gained by the simulation. The second, third and fourth natural frequencies are gained as 162.65 Hz (2nd bending), 228.68 Hz, (1st torsion) and 456.56 Hz (3rd bending) respectively. These modal shapes comprise of both bending and torsion.

Table 4.1: Natural frequencies of the beam

Mode	Natural frequencies (Hz)
1 (1 st Bending)	26.00
2 (2 nd Bending)	162.65
3 (1 st Torsion)	228.68
4 (3 rd Bending)	456.56

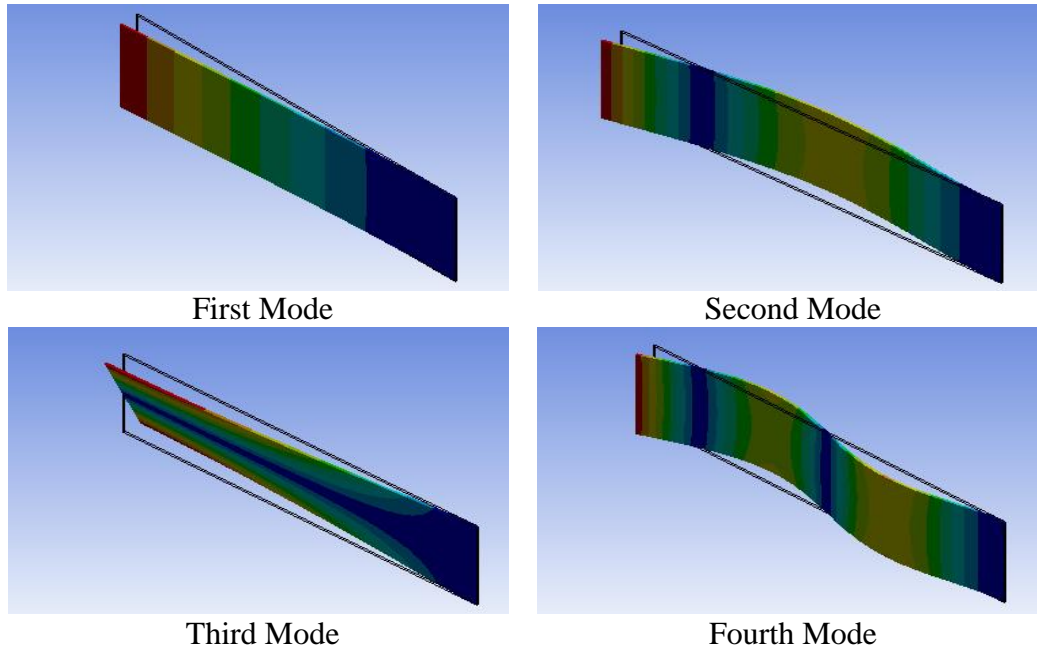
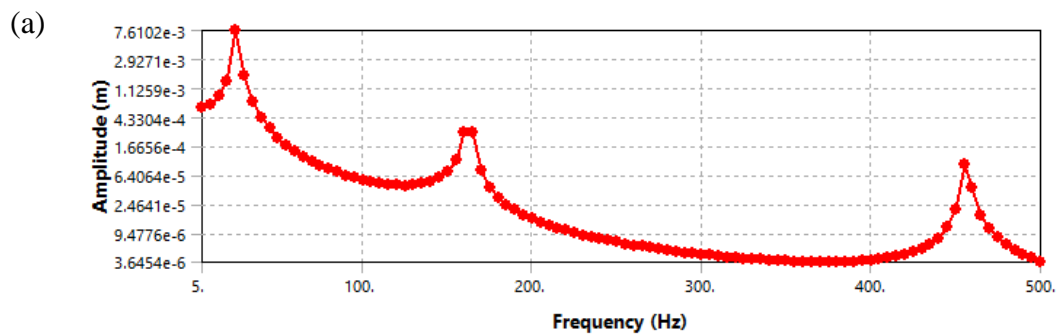


Figure 4.1: Mode shapes of the beam

The FRF graphs of displacement, velocity and acceleration generated by the harmonic response analysis are shown in Figure 4.2. From Figure 4.2, only the amplitudes generated by the bending modes can be show since they are more dominant in z-axis direction compared to the torsional modes which can be considered small. The acceleration FRF shows that, the pattern at which the amplitude is increases along the frequency approximately at 26.00, 162.65 and 456.56 Hz with amplitudes of 187.77, 288.02 and 737.53 m/s^2 respectively. It can be expected that, the acceleration would be the highest at 400 Hz and dropping down at 500 Hz. Further discussion, will considered the acceleration output only.



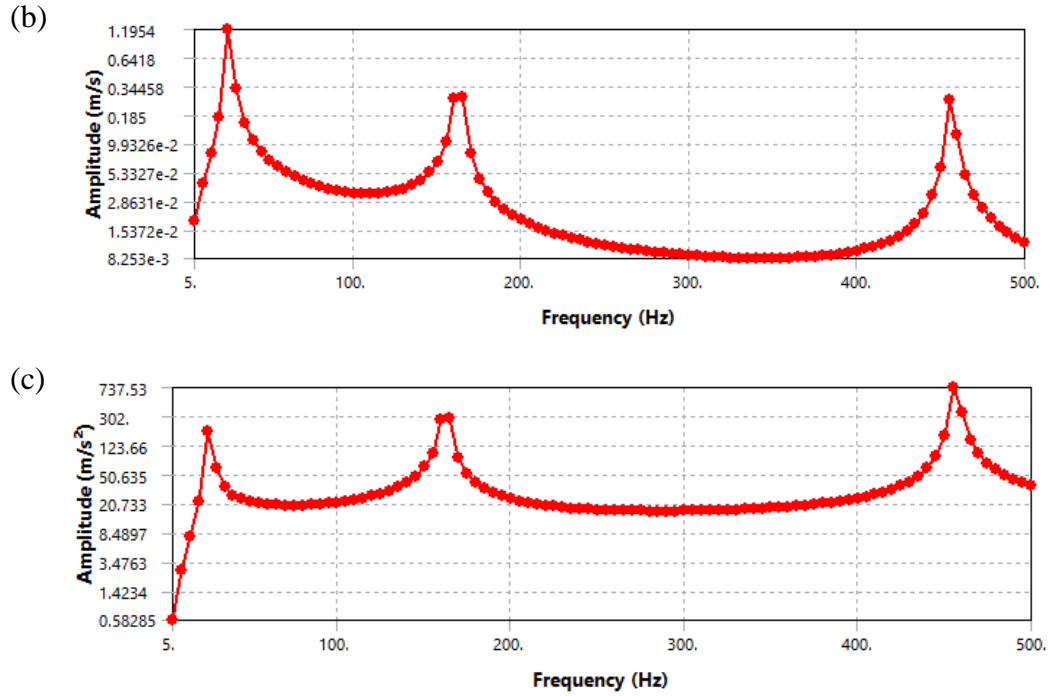
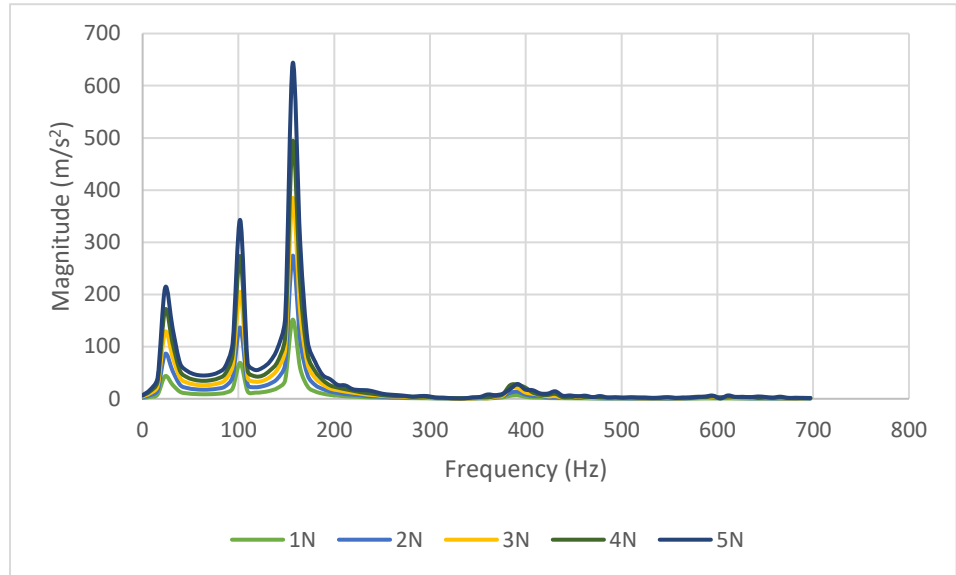


Figure 4.2: FRF of (a) displacement (b) velocity and (c) acceleration of the beam

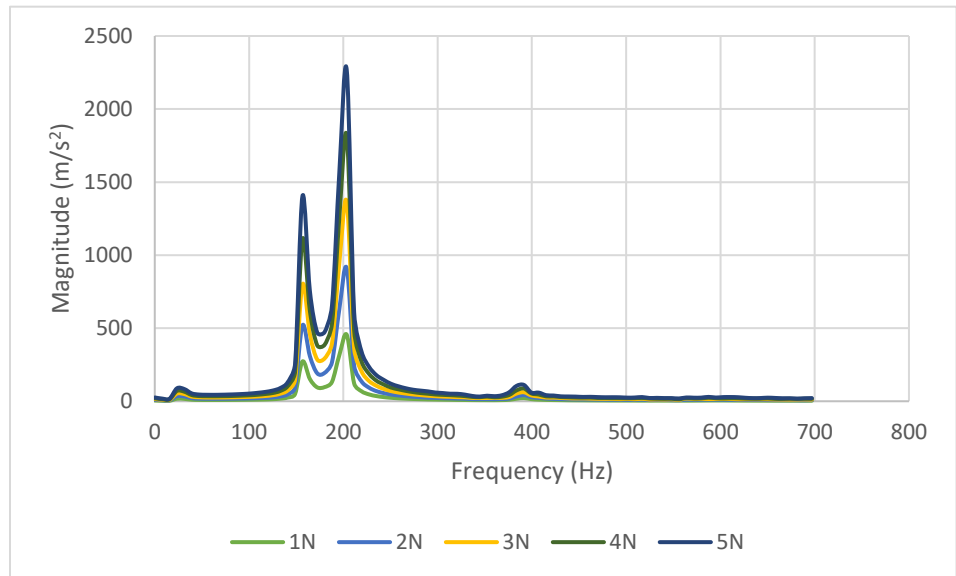
4.2.1.2 Transient analysis

In this section, all the results from ANSYS software are collected and Fast Fourier Transform (FFT) graph are plotted using EXCEL software. Figure 4.3 shows the FFT graphs of the beam at operating frequency of 100,200,300,400, and 500 Hz for input forces of $F_0 = 1,2,3,4,$ and 5 N. The deflection of the beam structure is shown in Figure 4.4. As shown in Figure 4.3 (a), the amplitude at 100 Hz increased linearly with the increased at excitation force of 1-5 N and the maximum amplitude achieved at 342.75 m/s². It also observed that, there are two peaks at 26.00 and 162.65 Hz due to the 1st and 2nd natural frequencies of the beam structure. Since the excitation at 100 Hz is closed to these natural frequencies, so that the beam is tend to excite at these natural frequencies simultaneously. The same effect is observed at 200 Hz and 300 Hz where at 200 Hz, the 2nd natural frequency of 162.65 Hz is tending to excite and 300 Hz, both 2nd and 4th natural frequencies are also tending to excite.

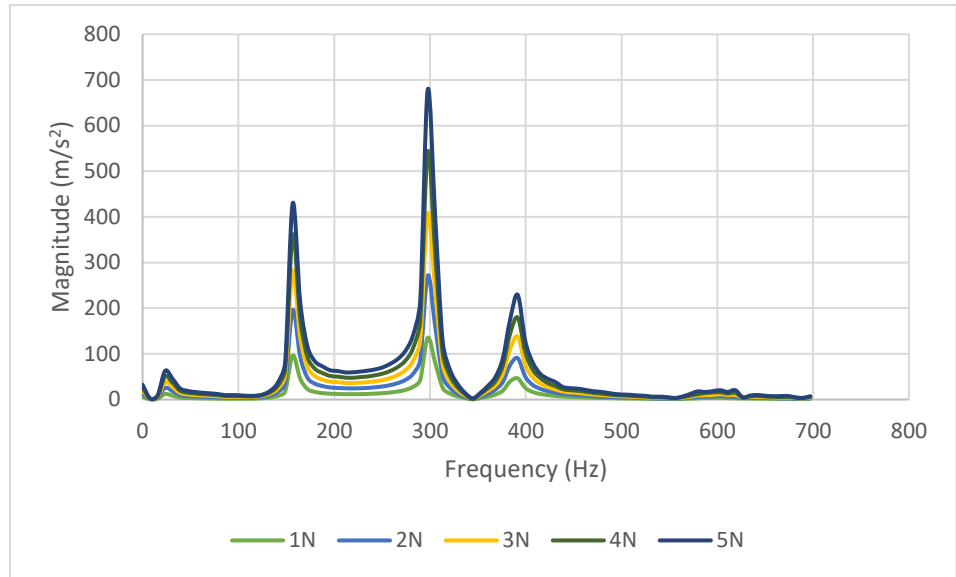
(a)



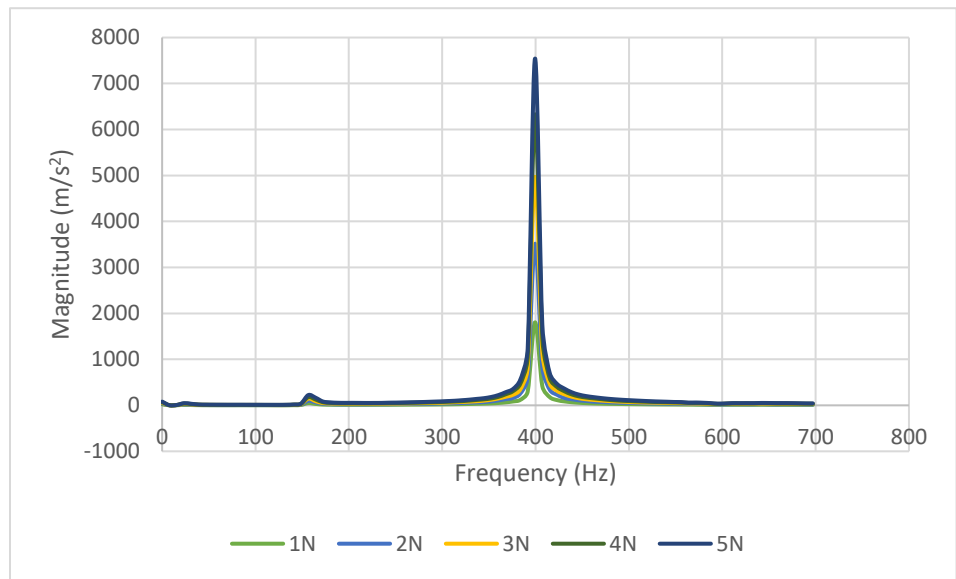
(b)



(c)



(d)



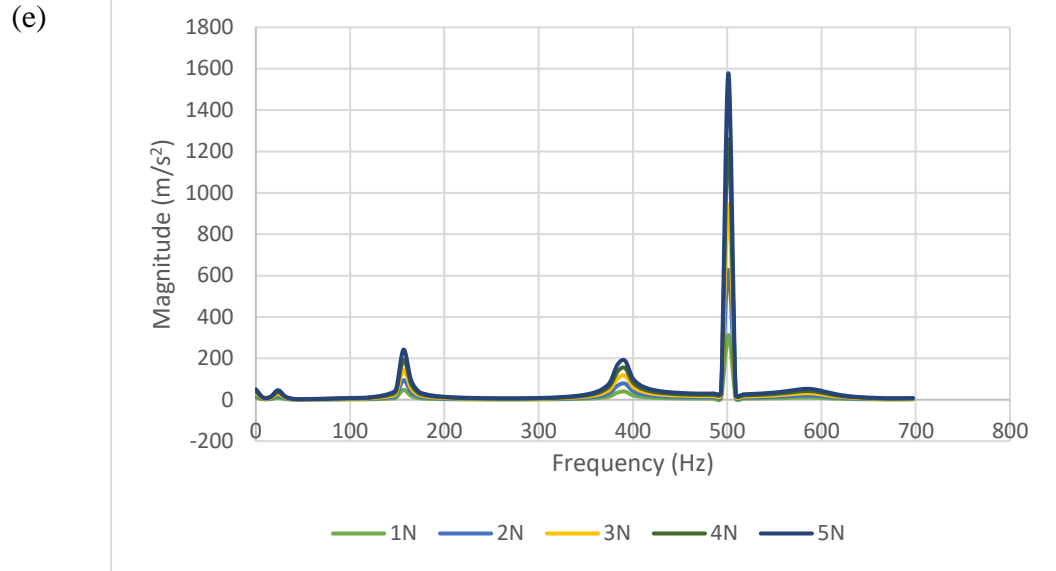


Figure 4.3: FFT acceleration of the beam with input forces at frequency (a) 100Hz (b) 200Hz (c) 300Hz (d) 400Hz and (e) 500 Hz

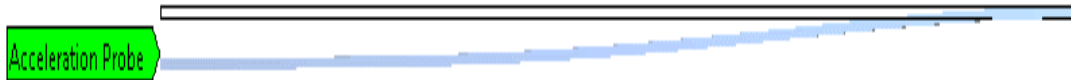


Figure 4.4: The deflection of the beam at 300 Hz for input force 1 N

For clear observation of the peak acceleration for each excitation frequency, the results are illustrated as in Figure 4.5. Referring to Figure 4.5, as expected the lowest acceleration occurred at 100 Hz with maximum amplitude of 342.76 m/s^2 at 5 N and the highest acceleration occurred is at 400 Hz with amplitude of 7542.19 m/s^2 at 5 N of excitation force. In overall, these results are considered acceptable since it can be related to the FRF graph that has been obtained before in Figure 4.2. As shown in Figure 4.5, the acceleration for 100 and 300 Hz are low as they are far away from the natural frequencies as shown in Figure 4.2. For 200, 400 and 500 Hz they are closed to the 2nd (162.65 Hz) and 4th (456.56 Hz) natural frequencies of the beam which affecting the amplitudes at the excitation frequencies. However, the amplitude values determine in this results are quite high and this is might due to the problems of analysis setting that being solved.

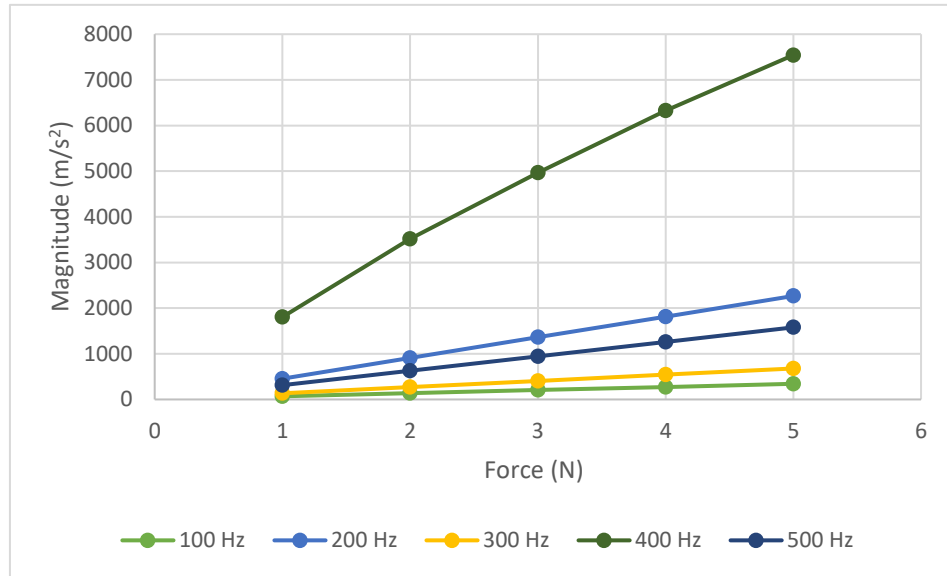


Figure 4.5: The results of acceleration of the beam at different operating frequencies and excitation forces

4.2.2. Beam with piezoelectric patches

4.2.2.1. Modal and harmonic response analysis

The results of the modal analysis at the beam with piezoelectric patches are tabulated in Table 4.2 and the mode shapes are shown in Figure 4.6. In this simulation, the beam and piezoelectric patches deformed together while vibrating and produce a quite different results compared to beam alone in section 4.2.1. The natural frequency of the beam with piezoelectric patch resulted with first natural frequency of 13.53 Hz as 1 bending for the first mode. It is slightly low compare to the beam alone in Figure 4.1. The second, third and fourth natural frequencies are obtained as 142.53 Hz (2nd bending), 150.12 Hz (1st torsion), and 499.48 Hz (3rd bending) respectively.

Table 4.2: Natural frequencies of the beam with piezoelectric patches

Mode	Natural frequency (Hz)
1 (1 st bending)	13.53
2 (2 nd bending)	142.53
3 (1 st torsion)	150.12
4 (3 rd bending)	499.48

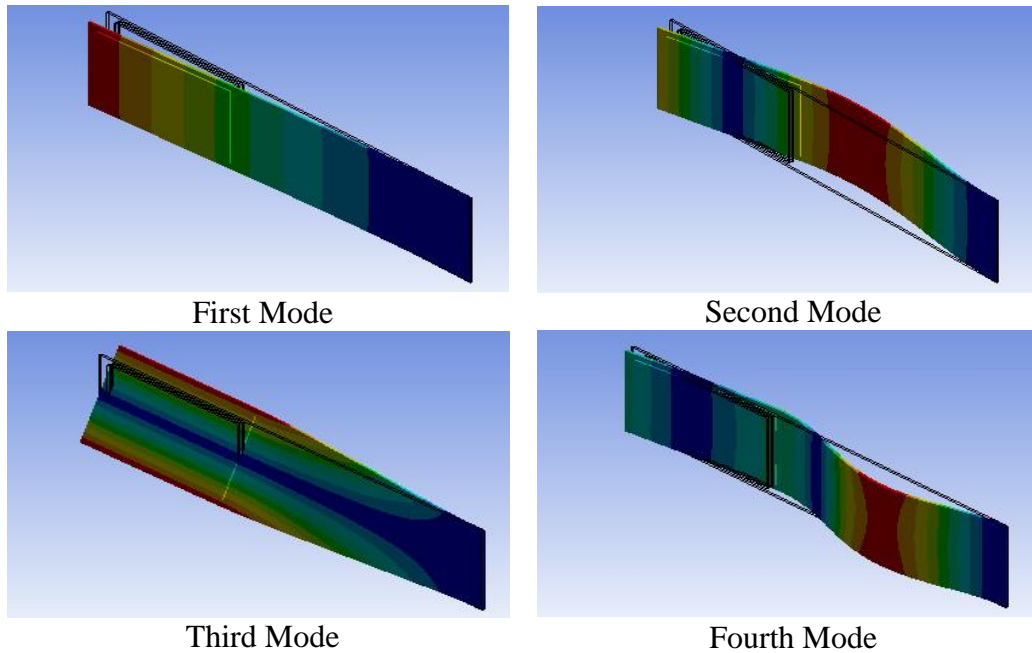


Figure 4.6: Mode shapes of the beam with piezoelectric patches

Similar to the FRF in Figure 4.2, the FRF for the beam piezoelectric patches only highlighted the natural frequencies for the bending modes as they are more dominant in z-axis direction. The FRF graphs of displacement, velocity and acceleration generated by the harmonic response analysis are shown in Figure 4.7. The acceleration FRF shows a pattern at which the amplitude increases with the increase in frequency, approximately at 13.53, 142.53 and 499.48 Hz the amplitudes of 72.41, 196.18 and 5289.50 m/s², respectively.